

SUPPORTING INFORMATION

Non-aggregating Solvatochromic Bipolar Benzo[*f*]quinolines and Benzo[*a*]acridines for Organic Electronics

Atul Goel,^{a,*} Vijay Kumar,^a Salil Pratap Singh,^a Ashutosh Sharma,^a Sattey Prakash,^b
Charan Singh,^b R. S. Anand^b

^aDivision of Medicinal and Process Chemistry,
Central Drug Research Institute, CSIR, Lucknow 226001, India
E-mail: atul_goel@cdri.res.in

^bDepartment of Electrical Engineering,
Indian Institute of Technology, Kanpur 208016, India.

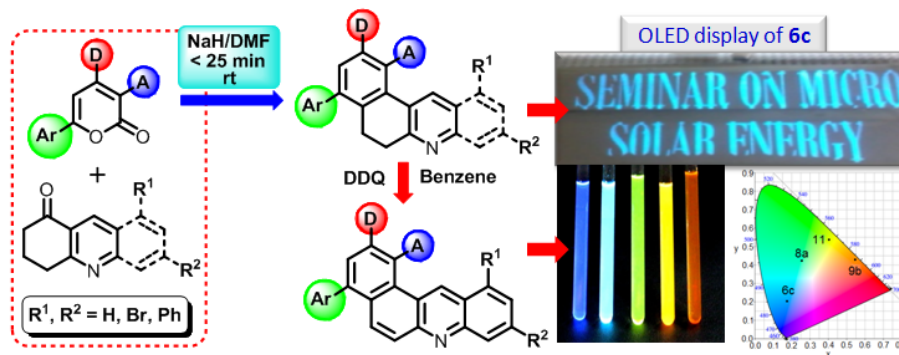


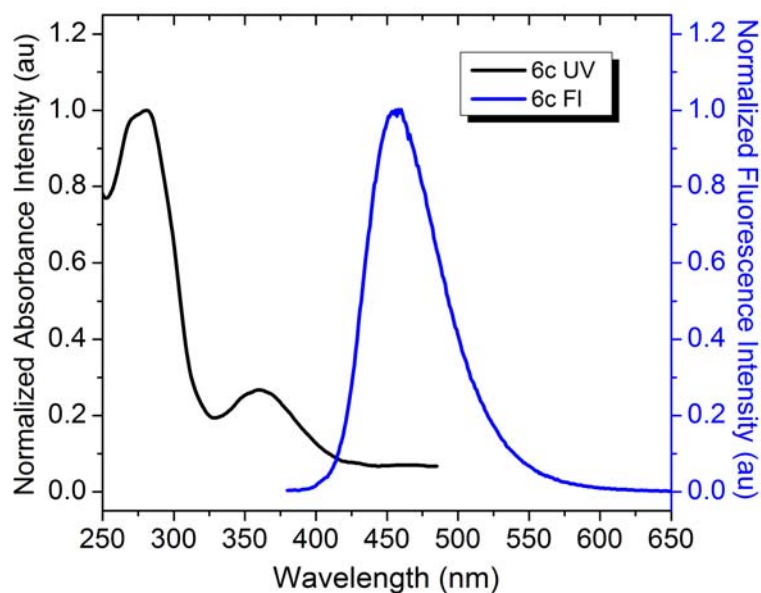
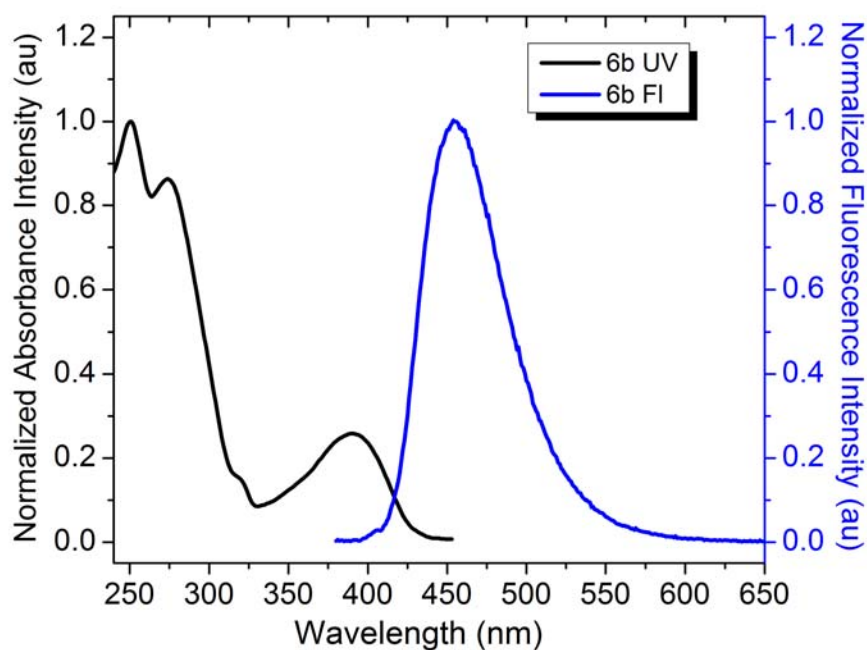
Table of Contents

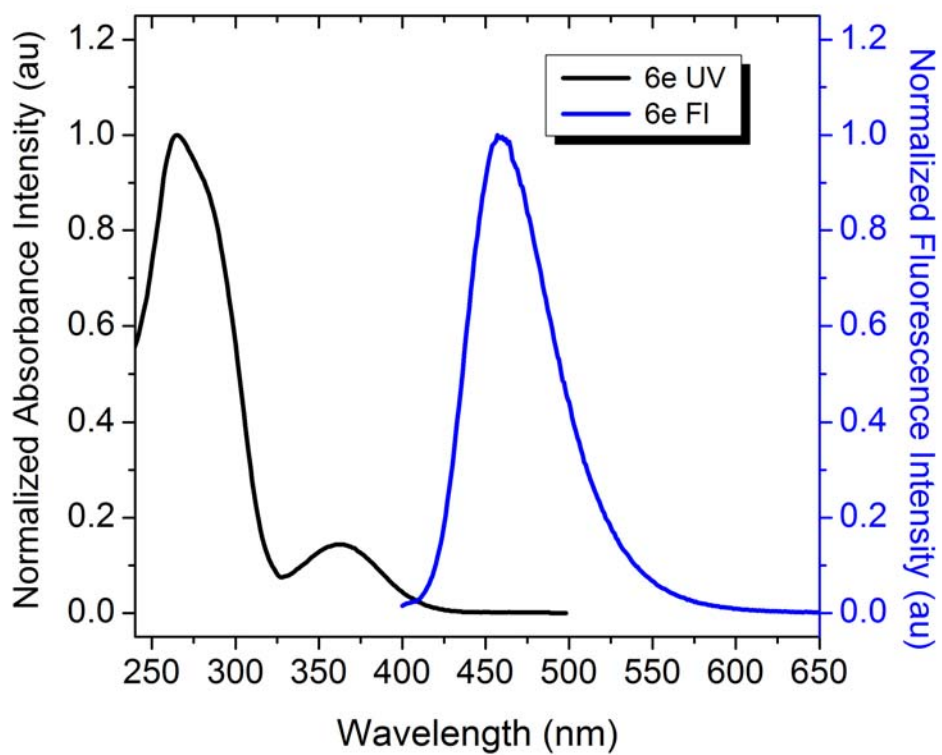
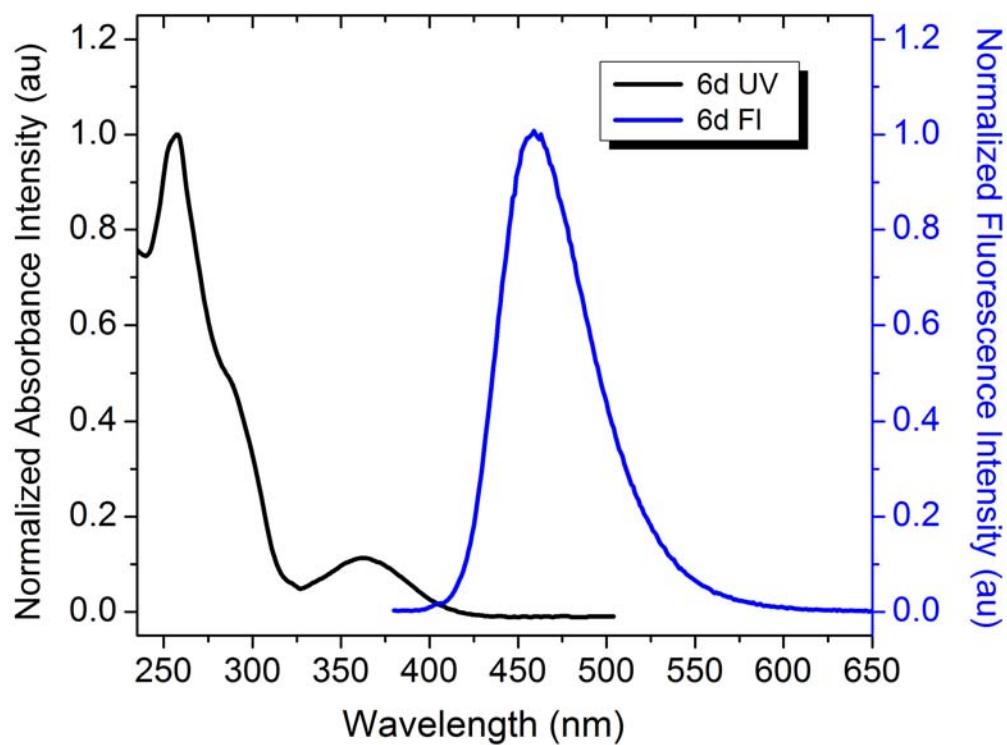
General information	S2
UV-fluorescence spectra of 6b-f , 10 , and 11	S3-S6
UV & FI Graphs of 6a in different solvents	S6
Cyclic Voltammograms of 6a-f , 8a,b , 9a , and 10	S7-S10
<i>I-L-V</i> characteristics (current density and luminance) of device 8a , 9b and 11	S10-S11
Copy of ¹ H and ¹³ C NMR of 6a-f , 8a,b , 9a,b , 10 and 11	S11-S23

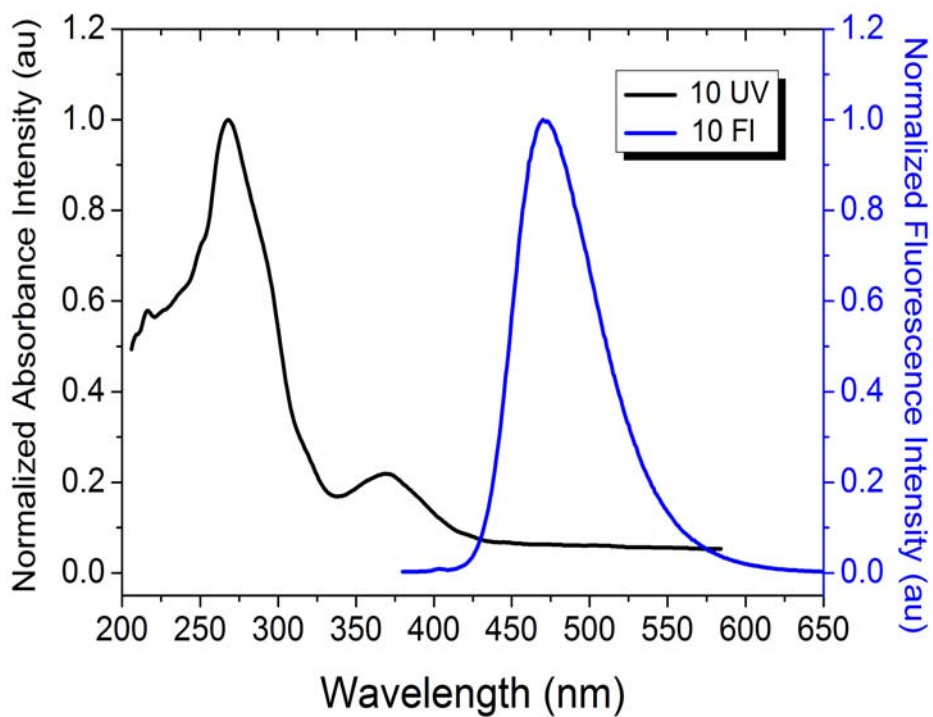
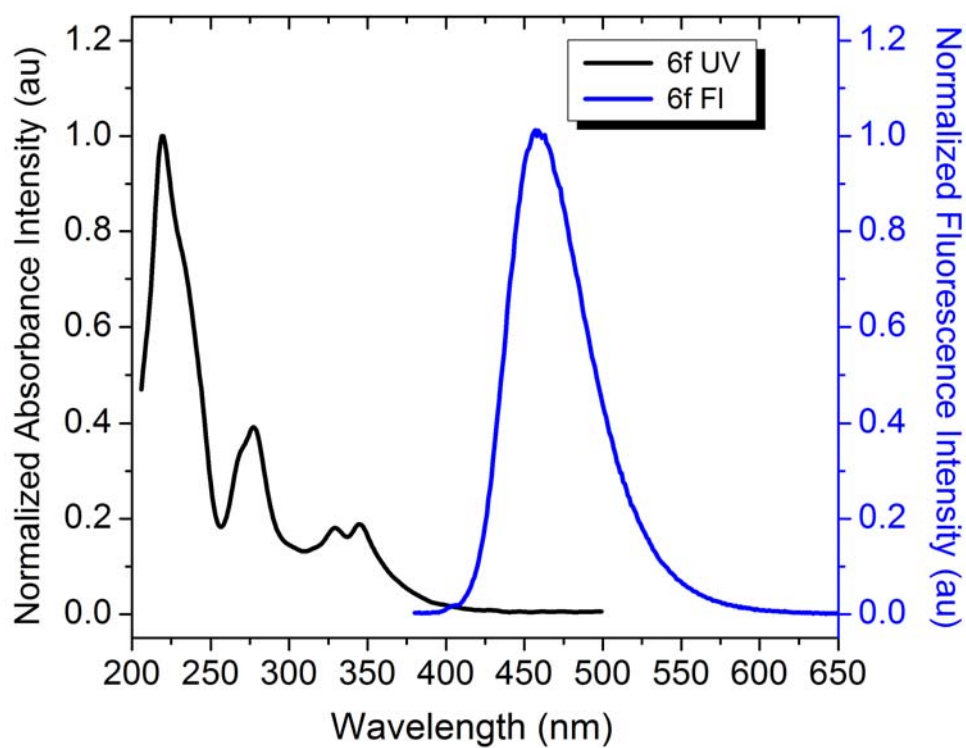
General: ^1H and ^{13}C NMR spectra were taken at 300 MHz. Chemical shift are reported in parts per million shift (δ -value) from Me_4Si (δ 0 ppm for ^1H) or based on the middle peak of the solvent (CDCl_3) (δ 75.00 ppm for ^{13}C NMR) as an internal standard. Signal pattern are indicate as s, singlet; d, doublet; dd, double doublet; t, triplet; m, multiplet. Coupling constant (J) is given in hertz. Infrared (IR) spectra were recorded in KBr disc and reported in wave number (cm^{-1}). The ESMS were recorded on MICROMASS Quadro-II LCMS system. The HRMS spectra were recorded as EI-HRMS on a JEOL system or as DART-HRMS (recorded as ES+) on a JEOL-AccuTOF JMS-T100LC Mass spectrometer having DART (Direct Analysis in Real Time) source. UV/Vis spectra were obtained using THF as solvent of choice having concentration is about 10^{-6} M. Fluorescence spectra were obtained using THF as solvent of choice, having concentration is about 10^{-6} M. Melting points were measured with melting point apparatus. Cyclic Voltammetry was done using Ag/AgCl as reference electrode. All the reactions were monitored by TLC and visualization was done with UV-light (254 nm).

UV and PL spectra of (6b-f, 10 and 11)

UV/Vis spectra were obtained with spectrometer with slit width of 1.5, using THF as solvent of choice having concentration 10^{-6} M. Photoluminescence spectra were obtained with slit width of 1.5, using THF as solvent of choice, having concentration 10^{-6} M.







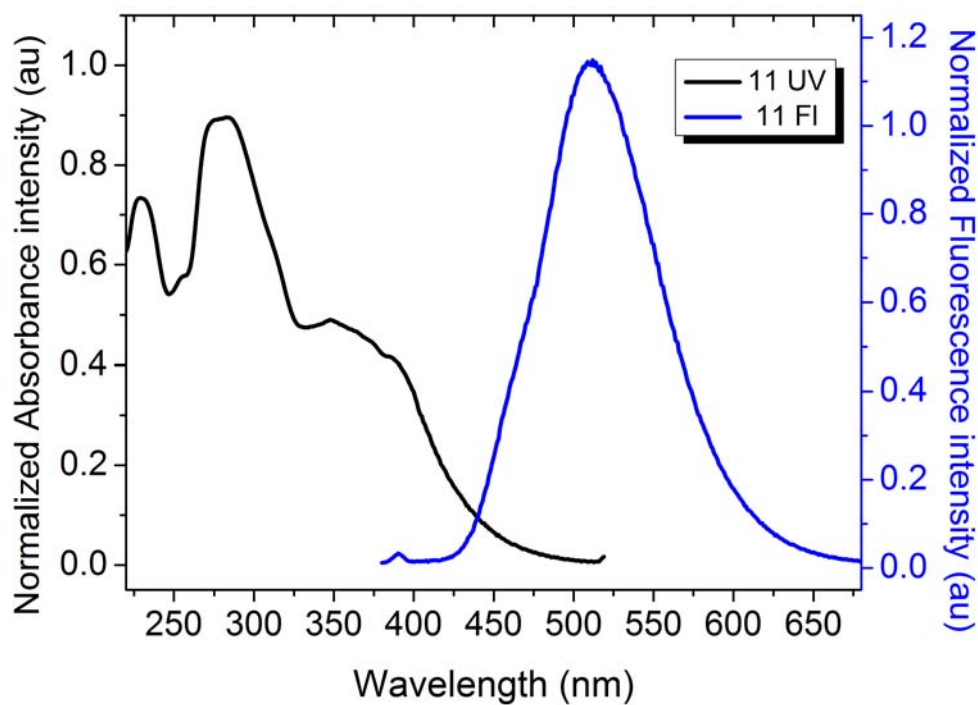


Figure S1. UV & FI Graphs of **6b-f**, **10** and **11** in THF

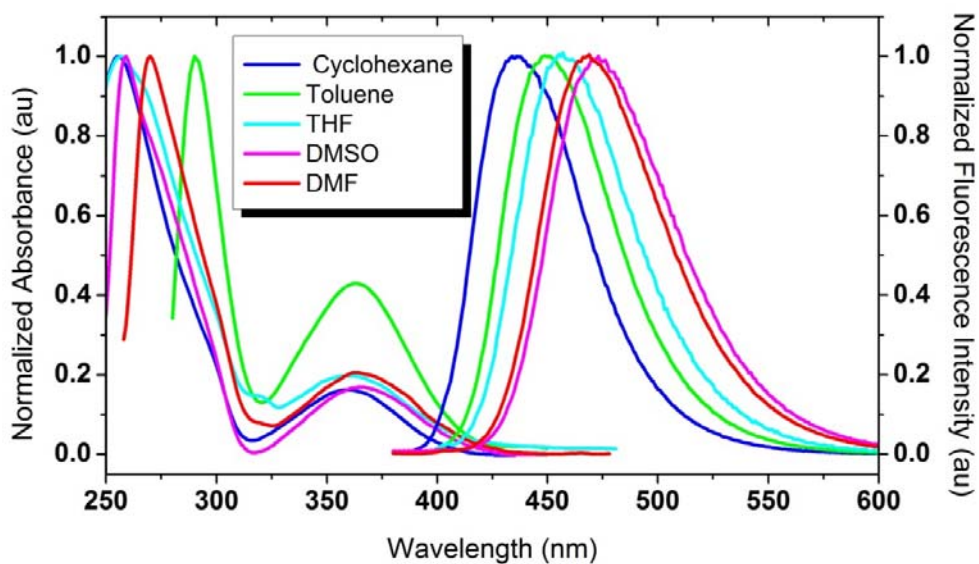


Figure S2. UV & FI Graphs of **6a** in different solvents (Inset shows the fluorescence images of solvatofluorochromism upon irradiation of **6a** in different solvents, from left to right: Cyclohexane, Toluene, THF, DMSO, and DMF).

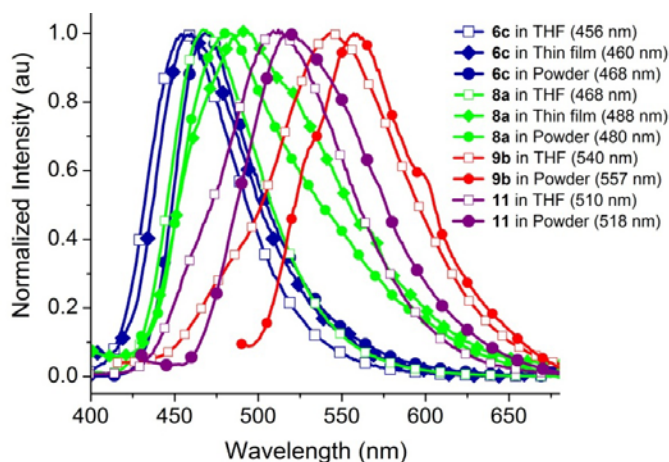
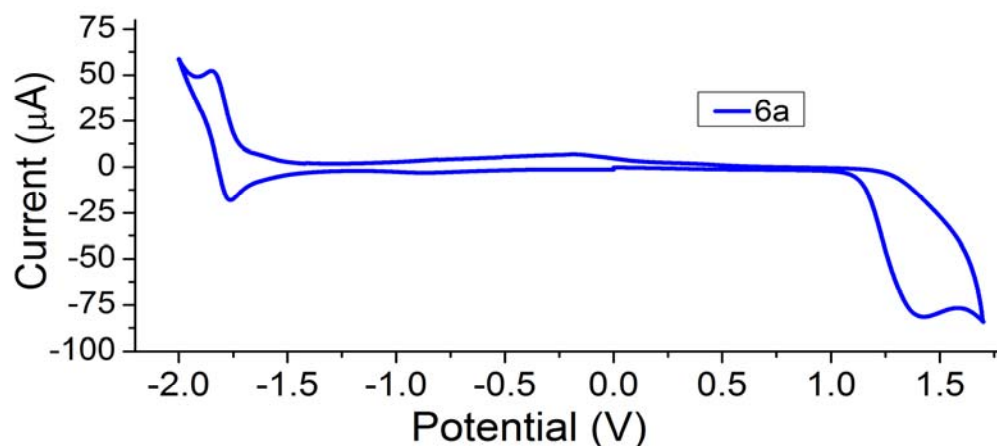
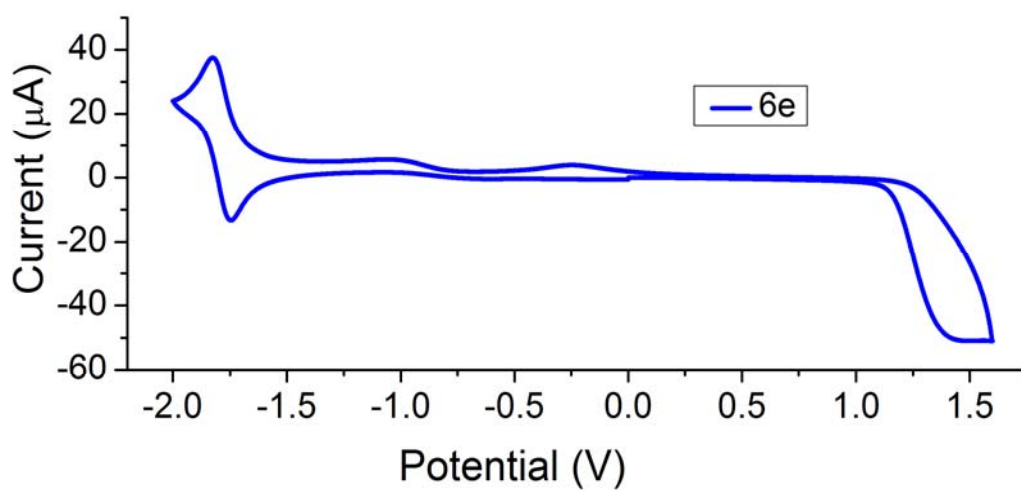
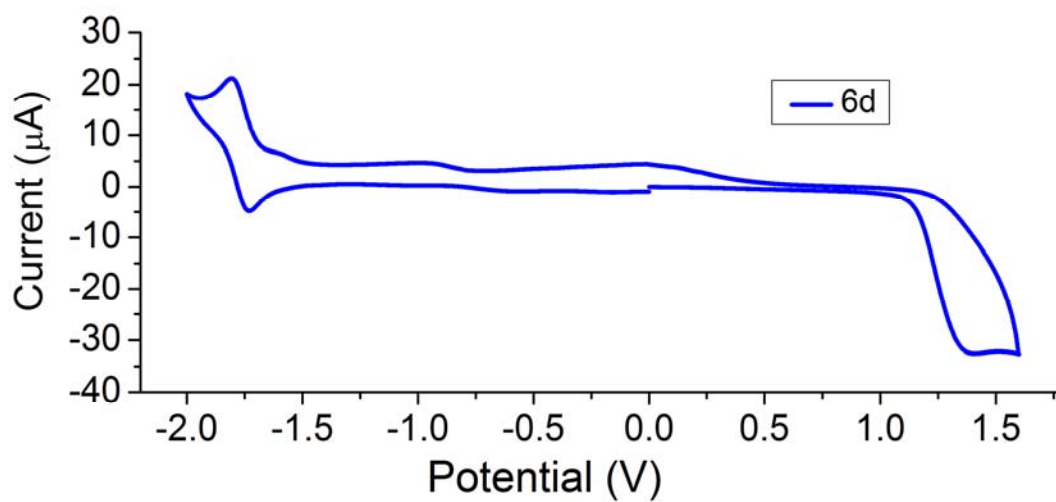
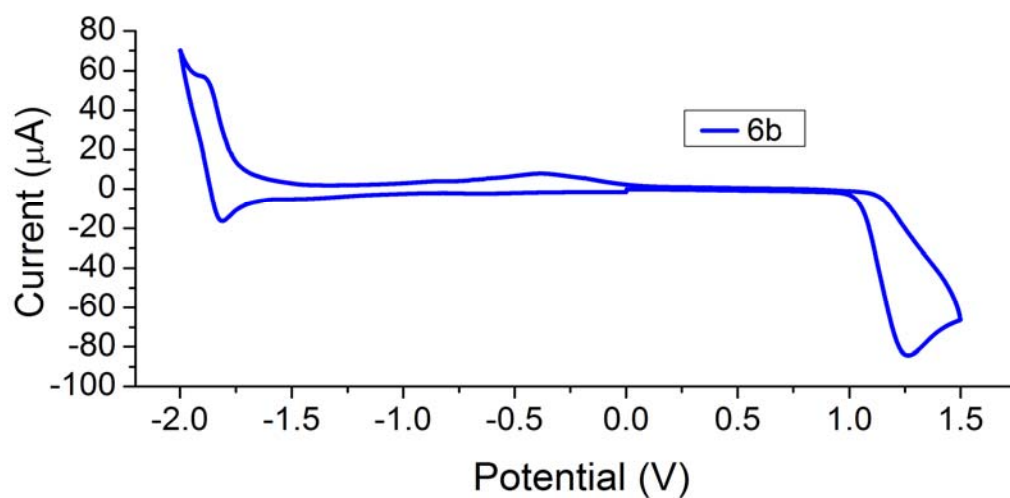


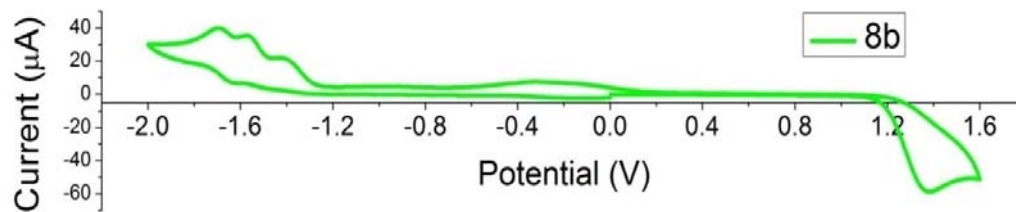
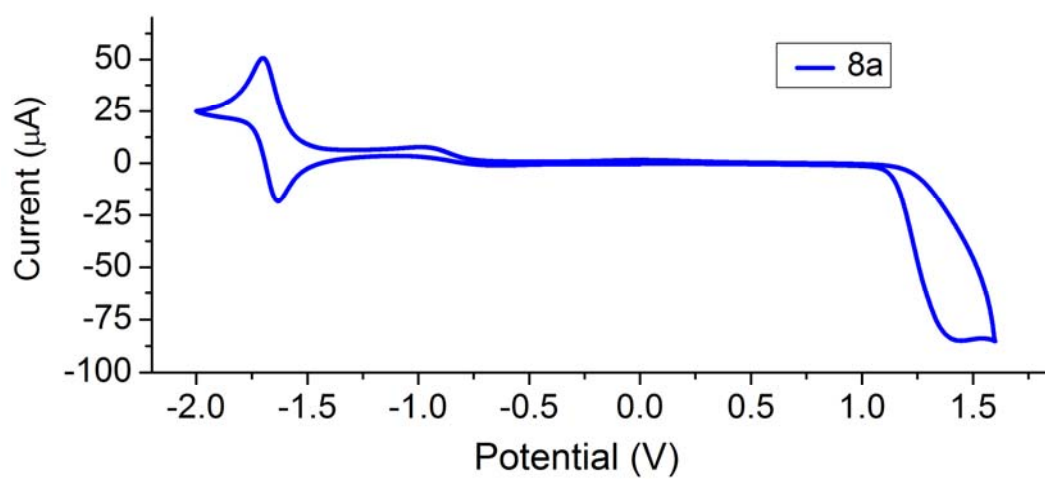
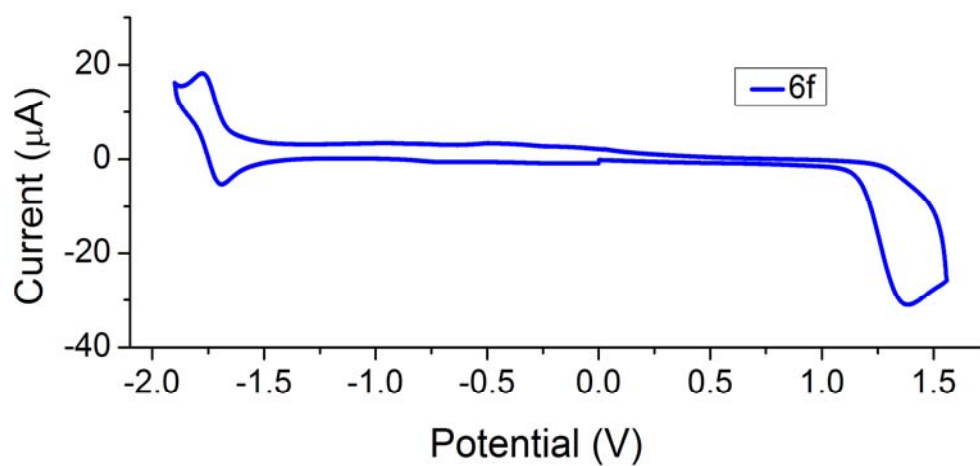
Fig. S3 Fluorescence spectra of **6c**, **8a**, **9b**, and **11** in powder form, **6c** and **8a** in the thin film

Electrochemical studies of **6a,b,d,e,f**, **8a,b**, **9a**, and **10**

The electrochemical studies were carried out to ascertain the redox behavior and the HOMO, LUMO energy values of the benzo[*f*]quinolines and benzo[*a*]acridines. Cyclic voltammetric measurements were performed in a three-electrode cell setup using Ag/AgCl as standard electrode and Pt disc as the working electrode, 2mM of N-heterocyclic compounds, and 0.2M of electrolyte tetrabutylammonium hexafluorophosphate (Bu_4NPF_6) dissolved in *N,N*-dimethylformamide. All the potentials were calibrated with ferrocene (Fc/Fc^+).







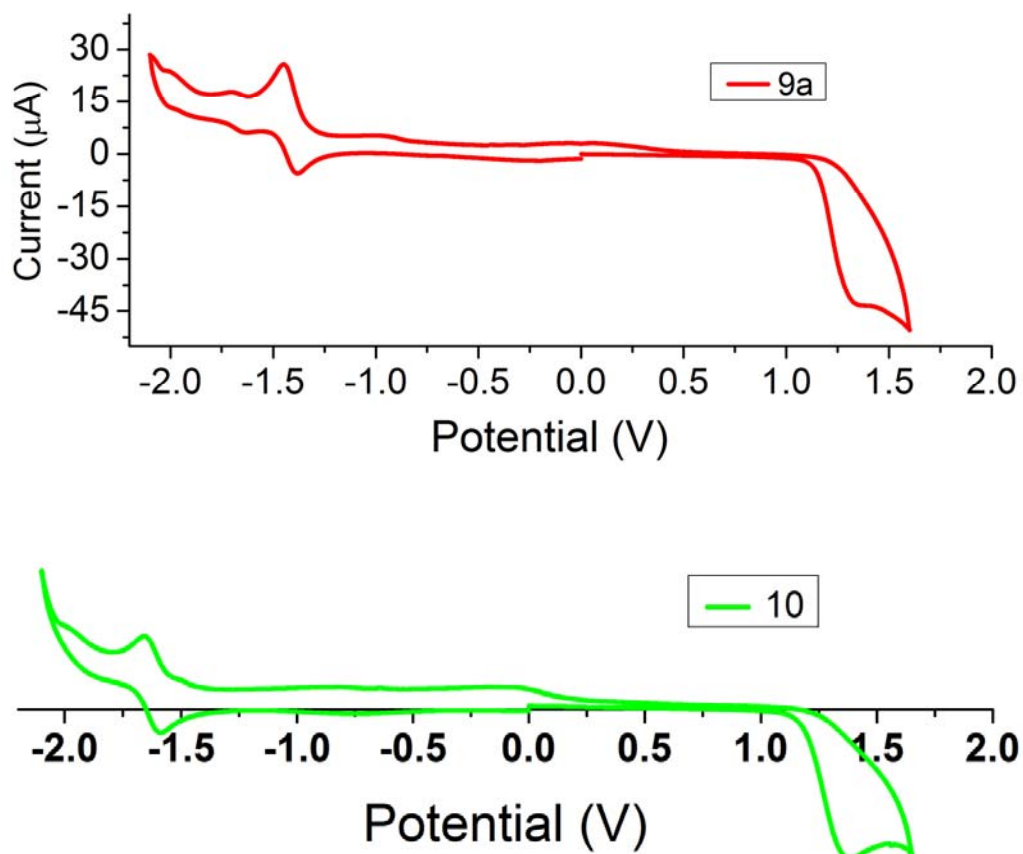


Figure S3. Cyclic Voltammograms of 6a,b,d,e,f, 8a,b, 9a, and 10

Single layer device characteristics of 6c (Diode 2) with configuration ITO/PEDOT:PSS(40 nm)/6c (100 nm)/LiF (0.7 nm)/Al (200 nm)

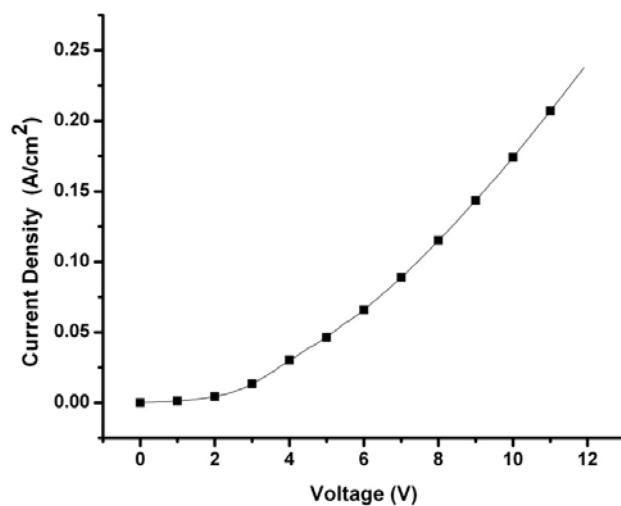


Figure S4. I - V characteristics of single layer device of 6c

Device characteristics of of **8a**, **9b**, and **11**

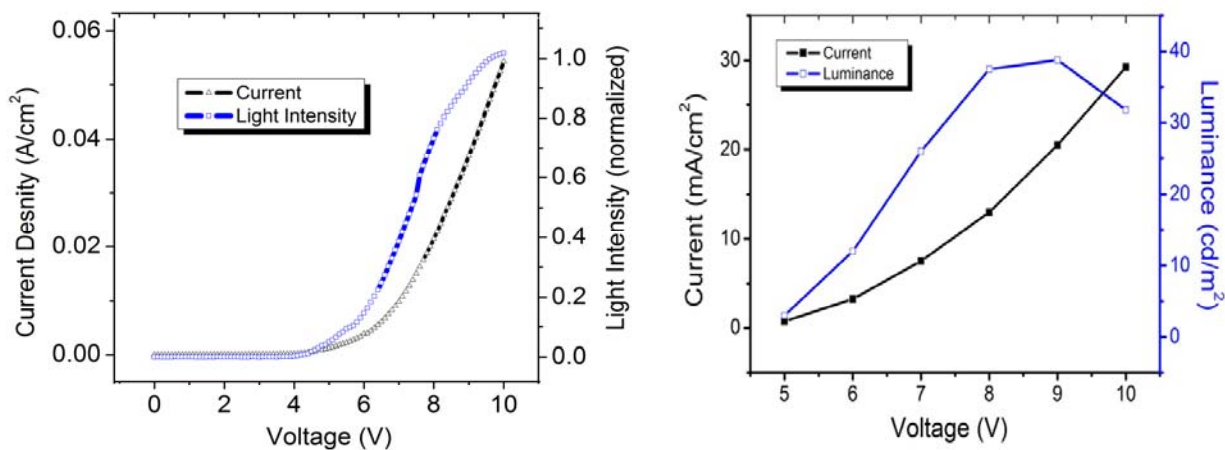


Figure S4. *I*-*L*-*V* characteristics of device of **8a**

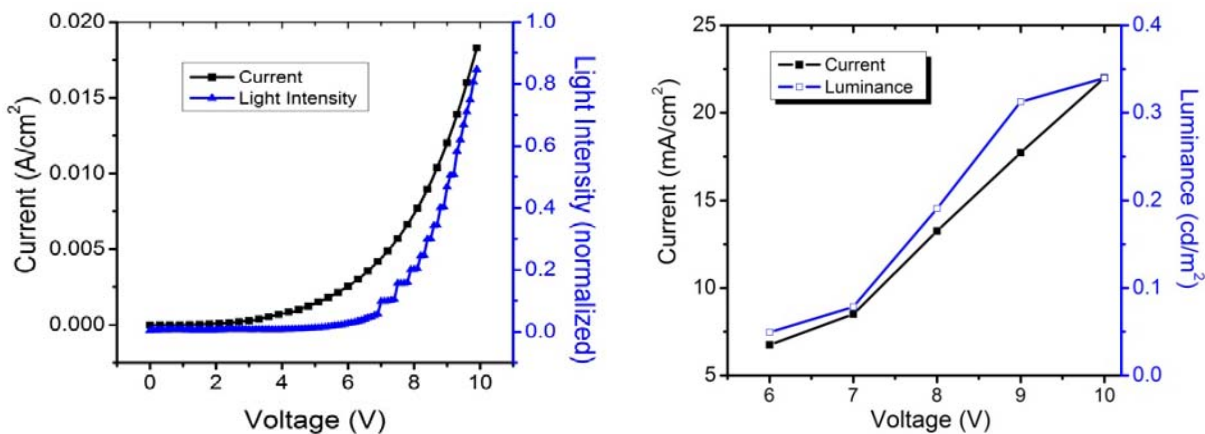


Figure S5. *I*-*L*-*V* characteristics of device of **9b**

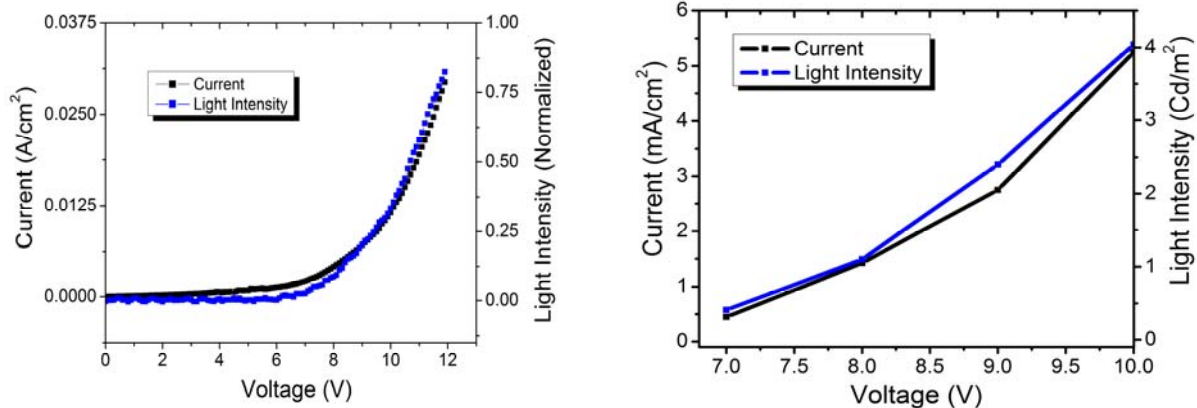


Figure S6. *I*-*L*-*V* characteristics of device of **11**

^1H and ^{13}C NMR Spectra of compounds

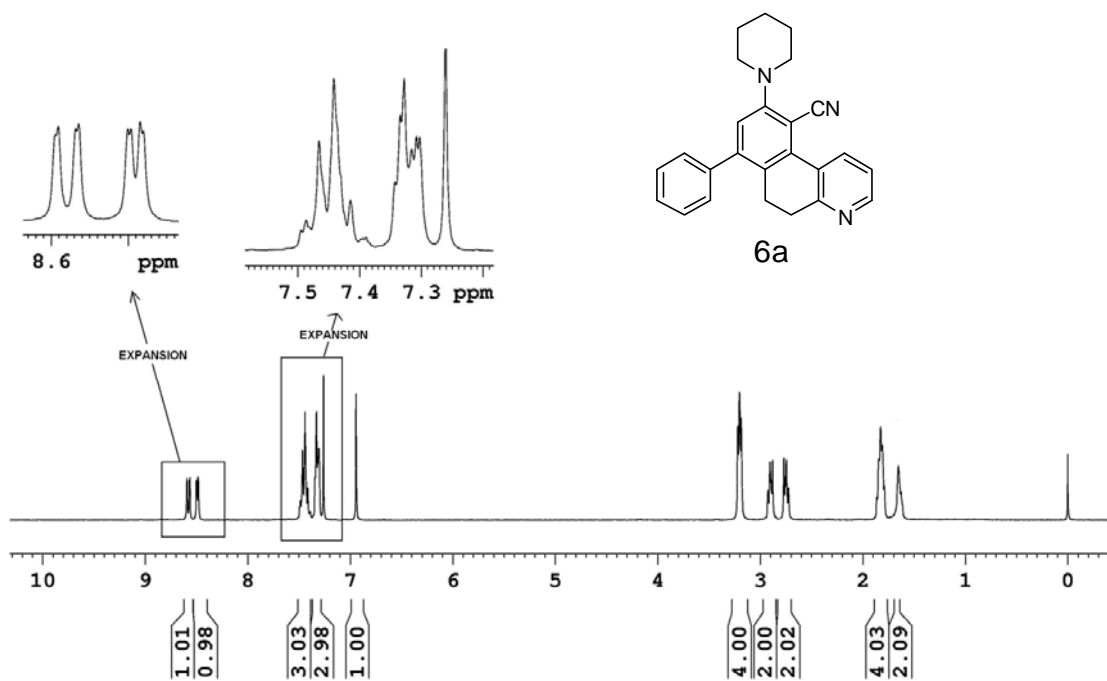


Figure S7. ^1H NMR spectrum of **6a** in CDCl_3

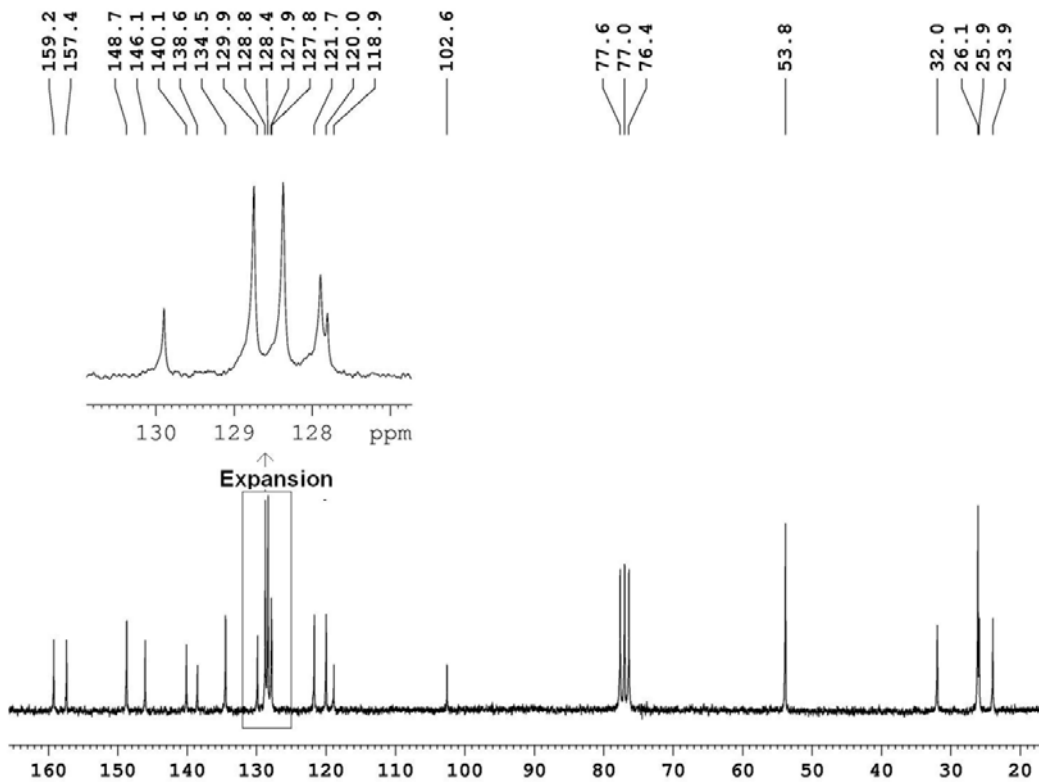
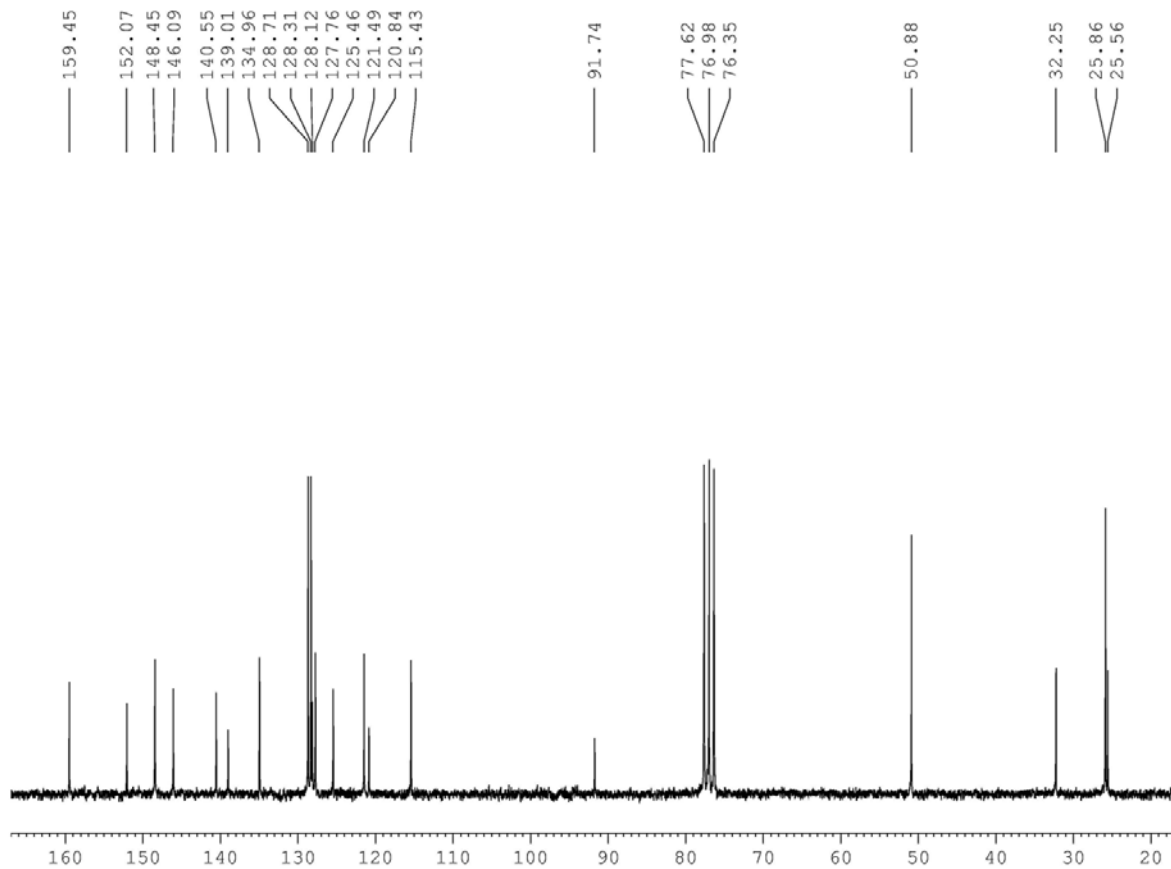
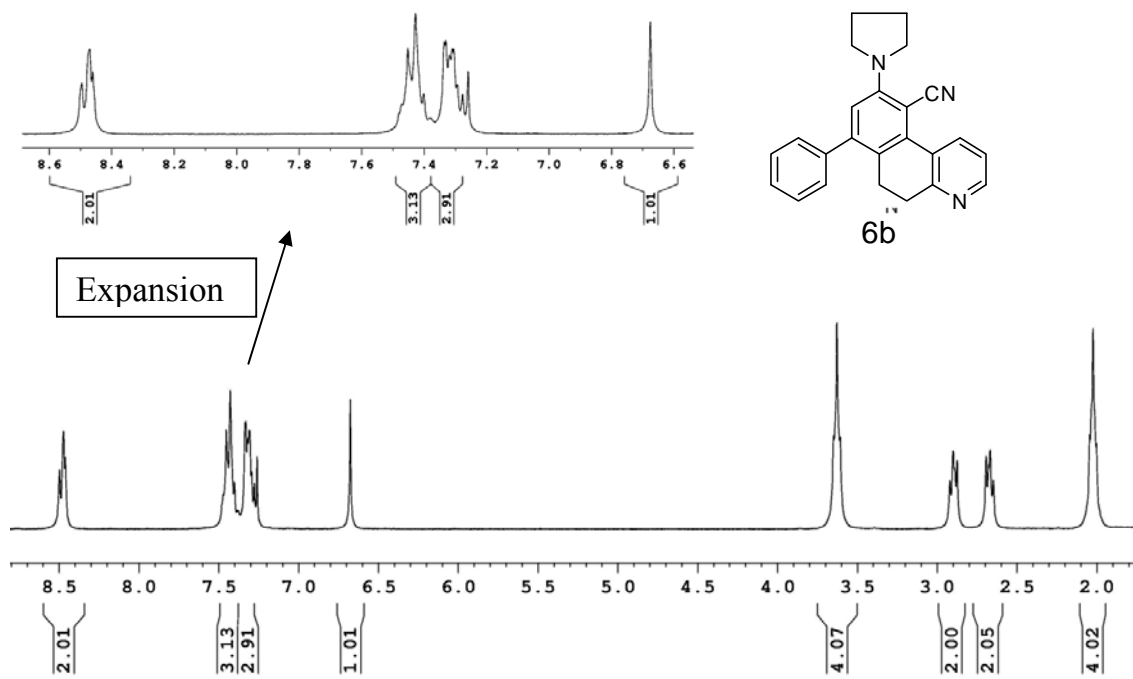


Figure S8. ^{13}C NMR spectrum of **6a** in CDCl_3



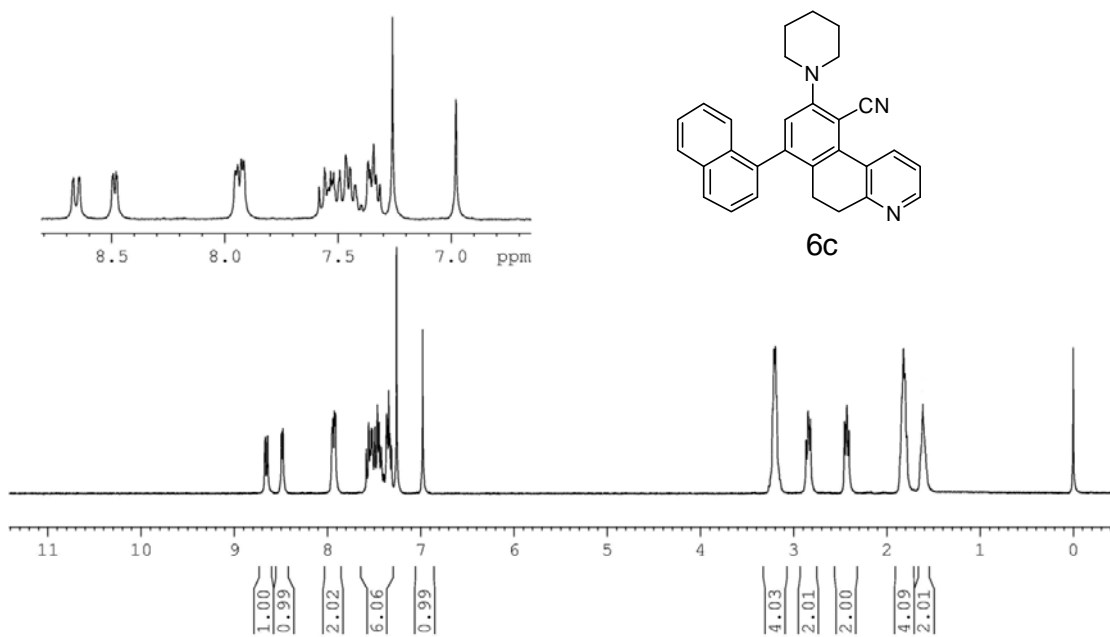


Figure S11. ¹H NMR spectrum of **6c** in CDCl₃

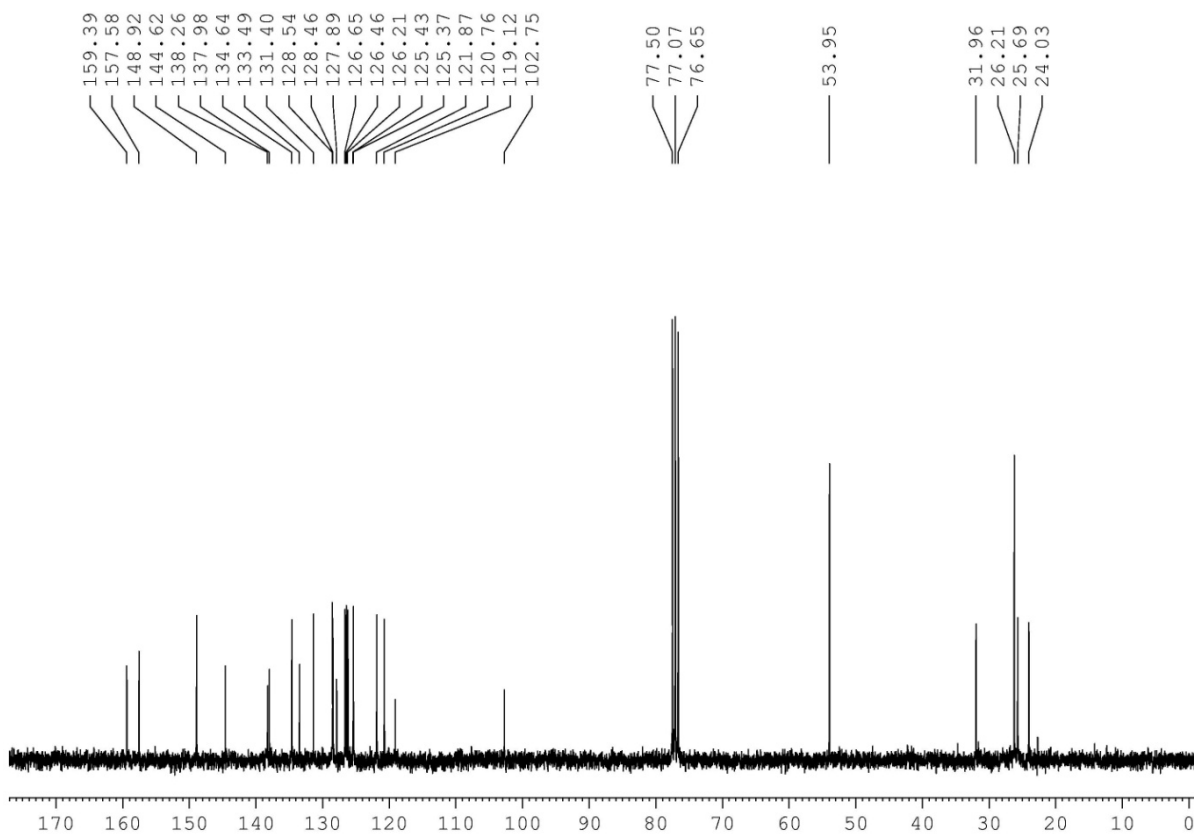


Figure S12. ¹³C NMR spectrum of **6c** in CDCl₃

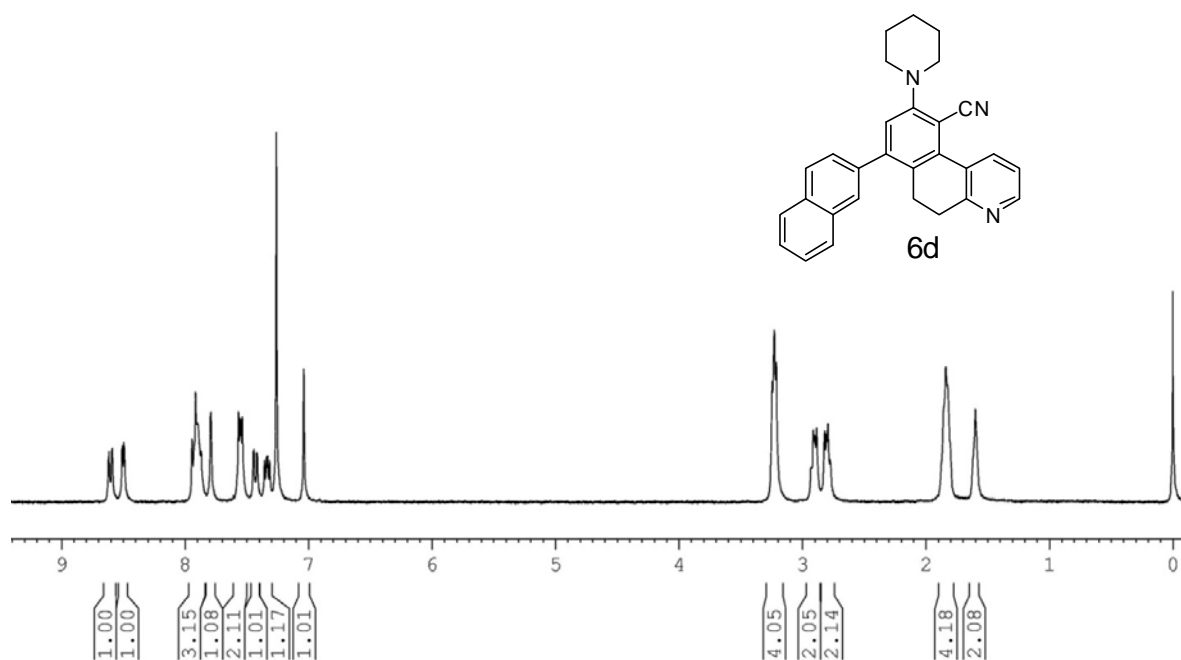


Figure S13. ¹H NMR spectrum of **6d** in CDCl₃

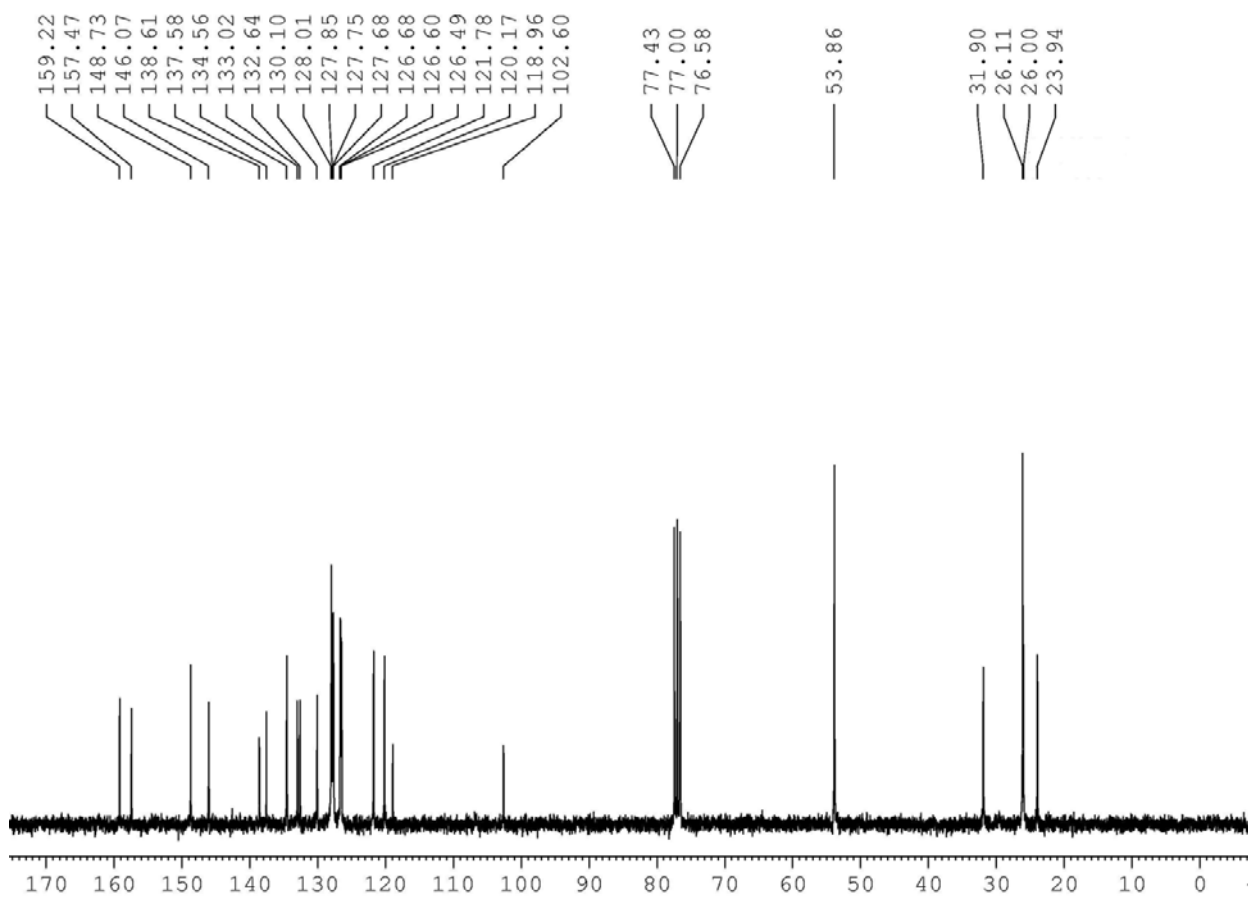


Figure S14. ¹³C NMR spectrum of **6d** in CDCl₃

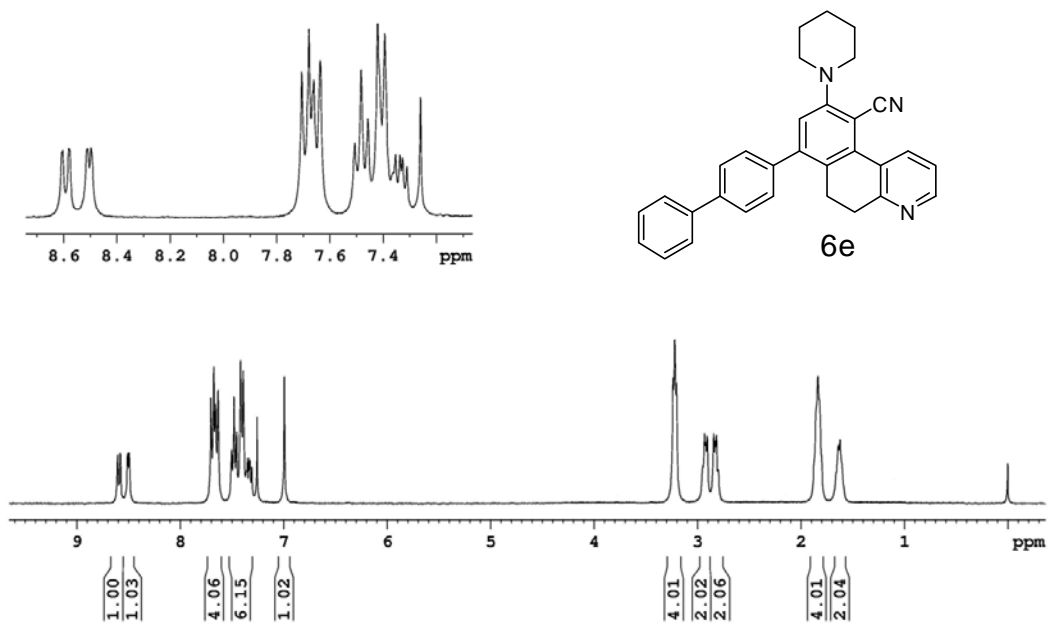


Figure S15. ^1H NMR spectrum of **6e** in CDCl_3

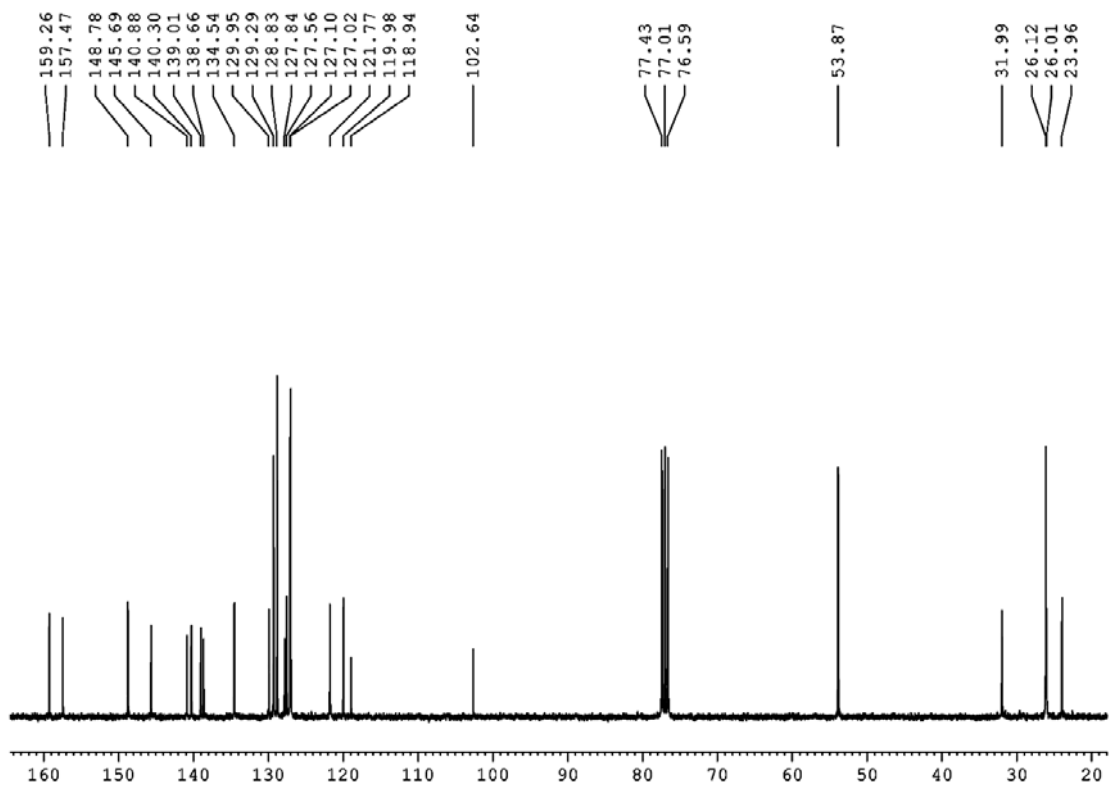
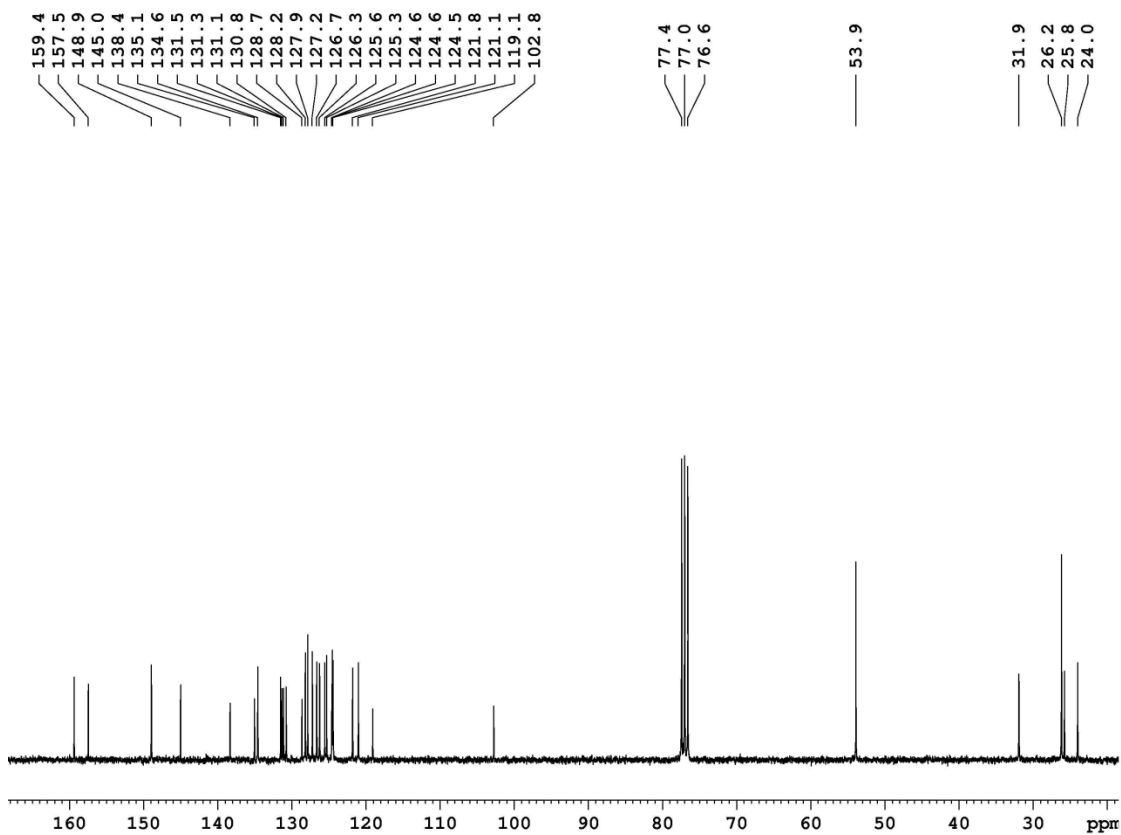
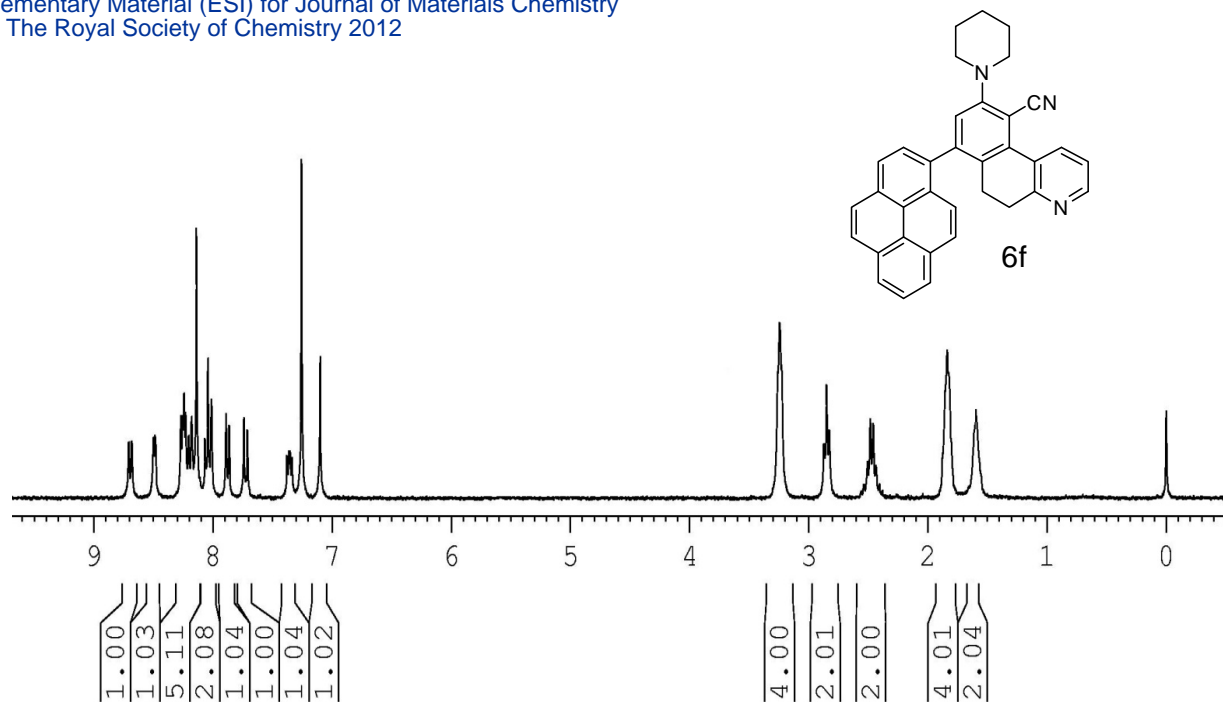


Figure S16. ^{13}C NMR spectrum of **6e** in CDCl_3



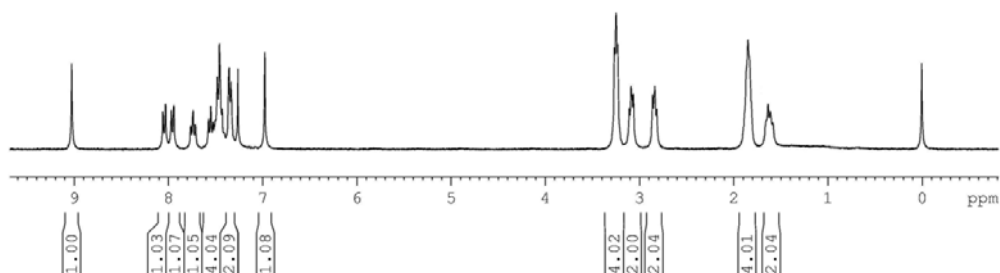
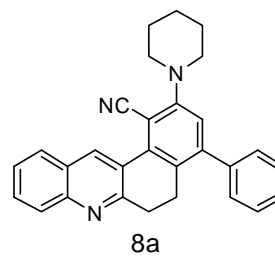


Figure S19. ¹H NMR spectrum of **8a** in CDCl₃

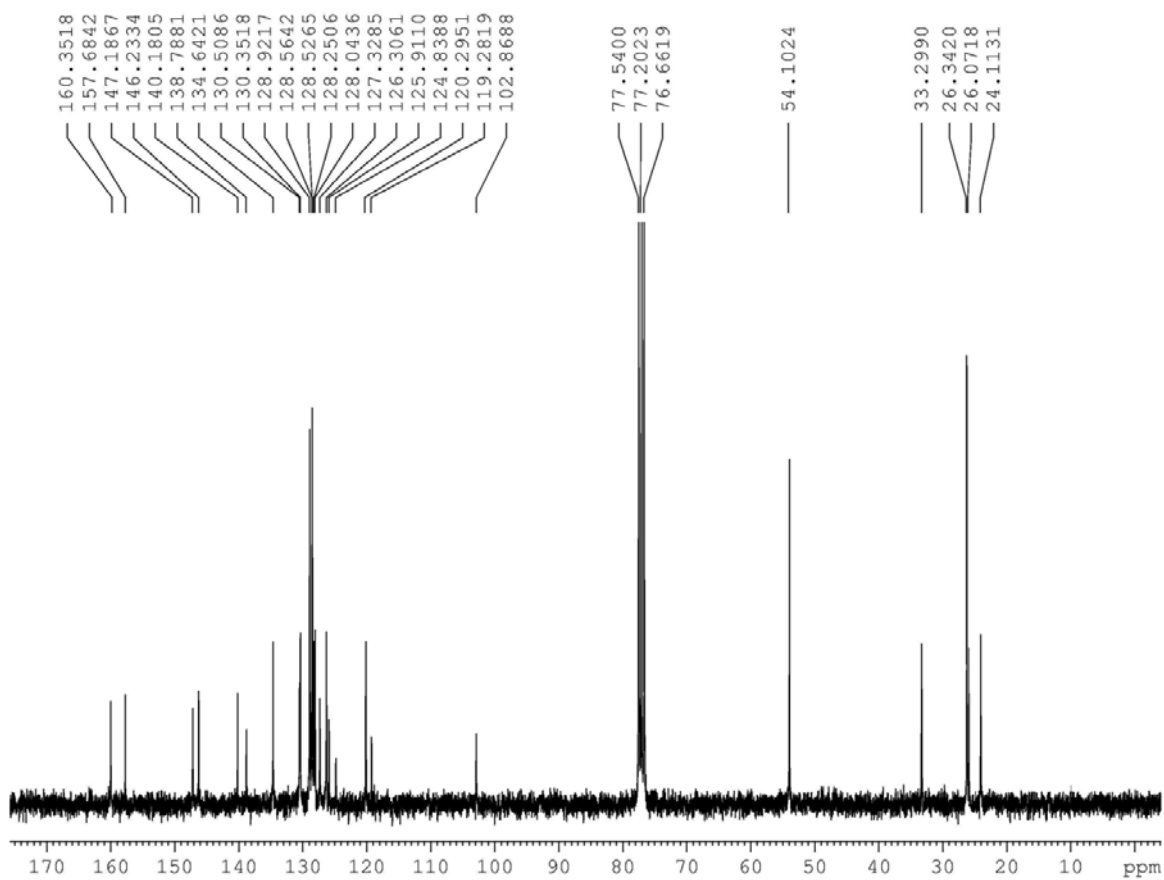


Figure S20. ¹³C NMR spectrum of **8a** in CDCl₃

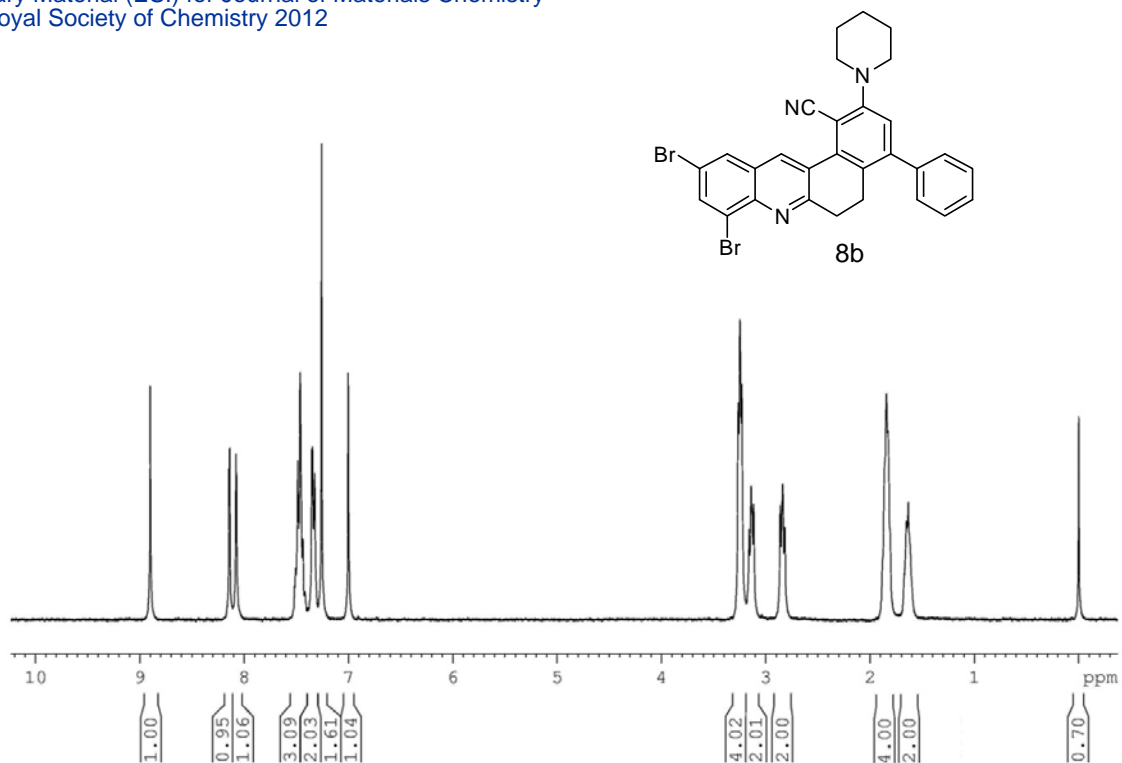


Figure S21. ¹H NMR spectrum of **8b** in CDCl₃

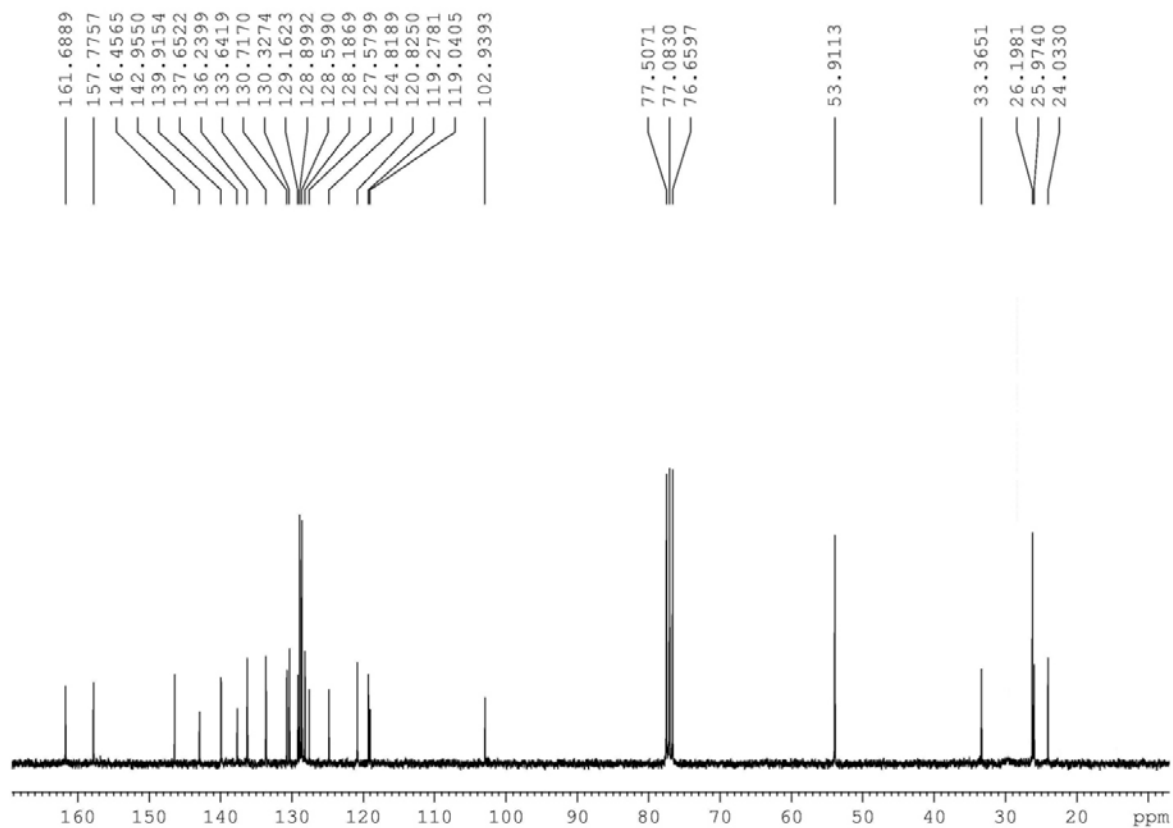
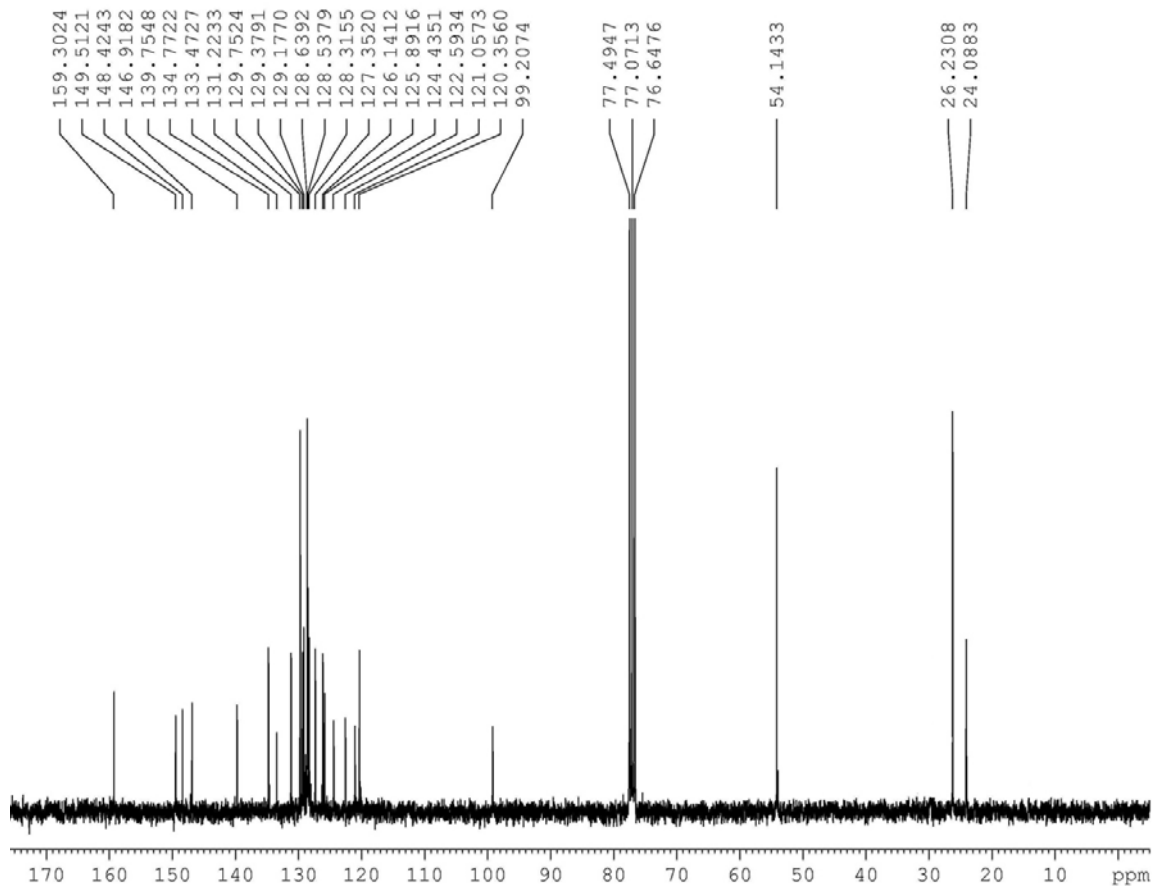
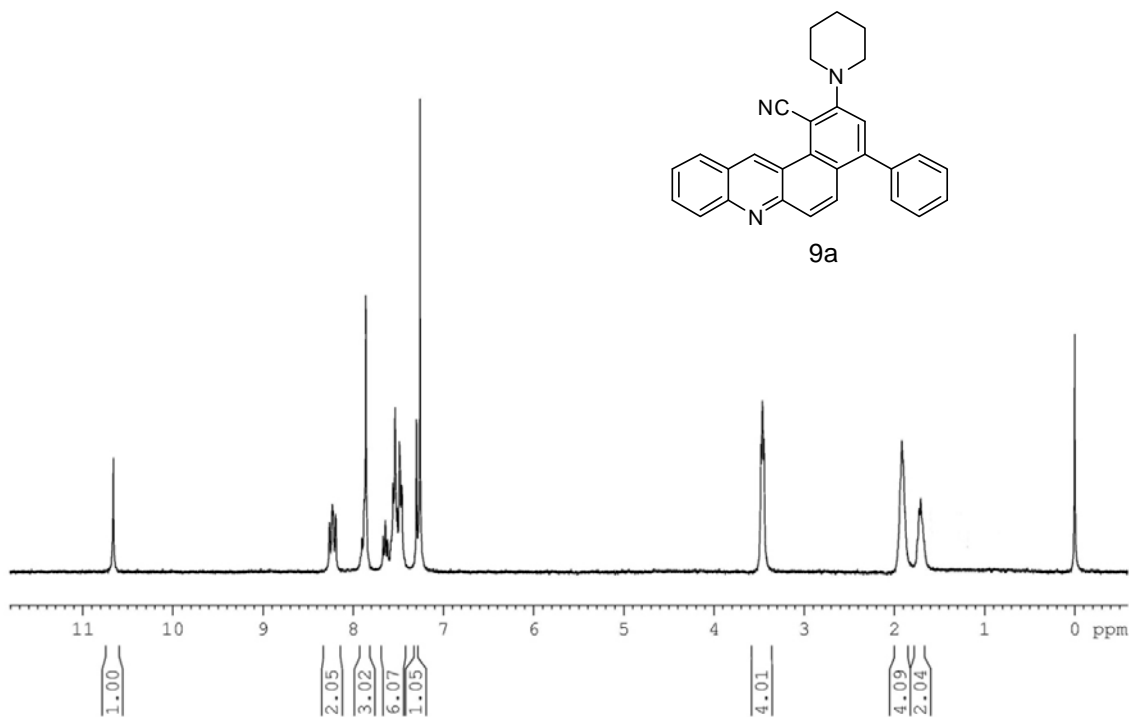


Figure S22. ¹³C NMR spectrum of **8b** in CDCl₃



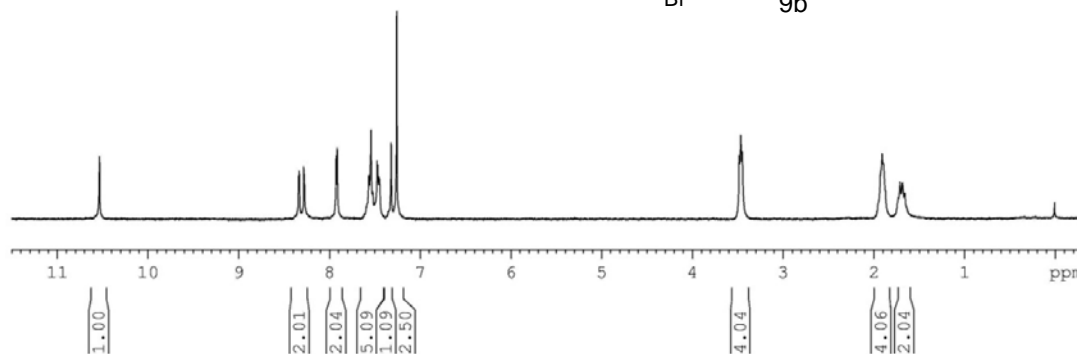
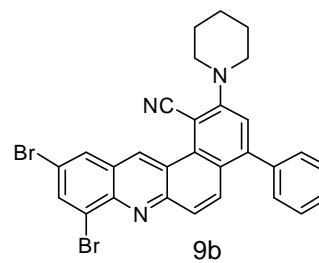


Figure S25. ^1H NMR spectrum of **9b** in CDCl_3

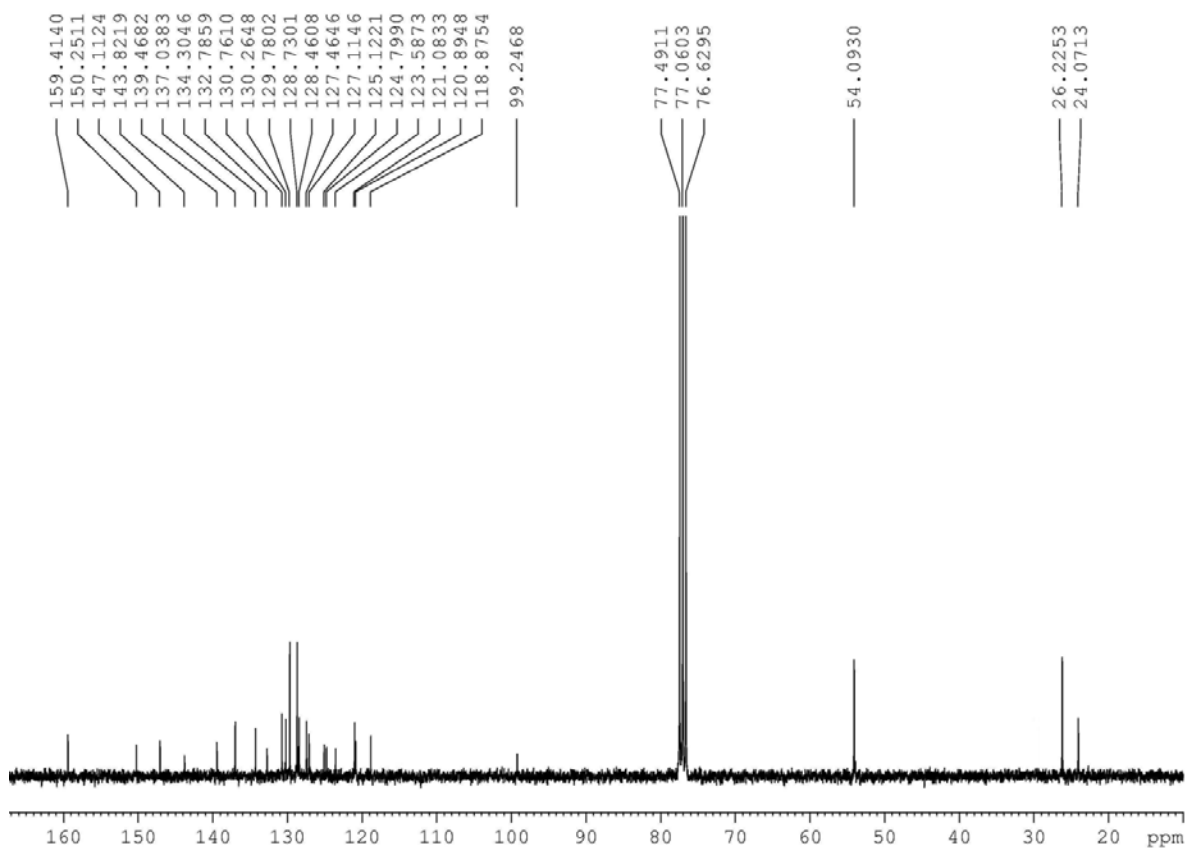
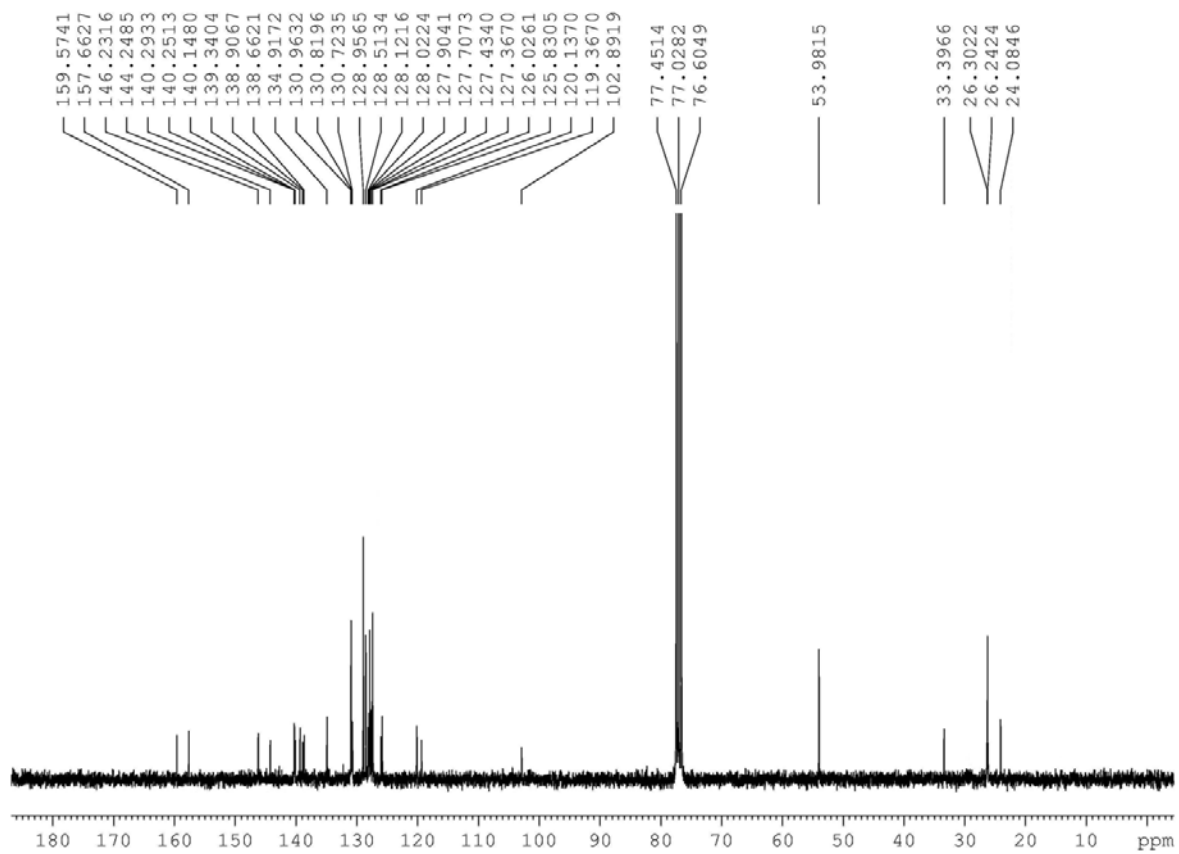
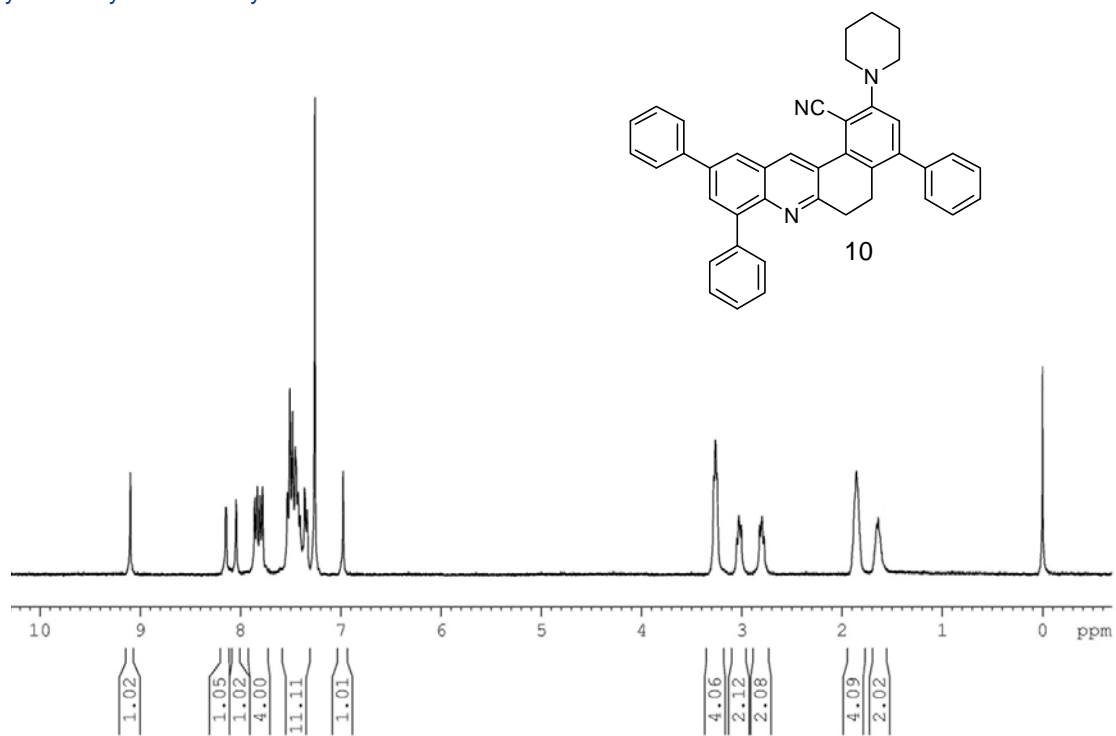


Figure S26. ^{13}C NMR spectrum of **9b** in CDCl_3



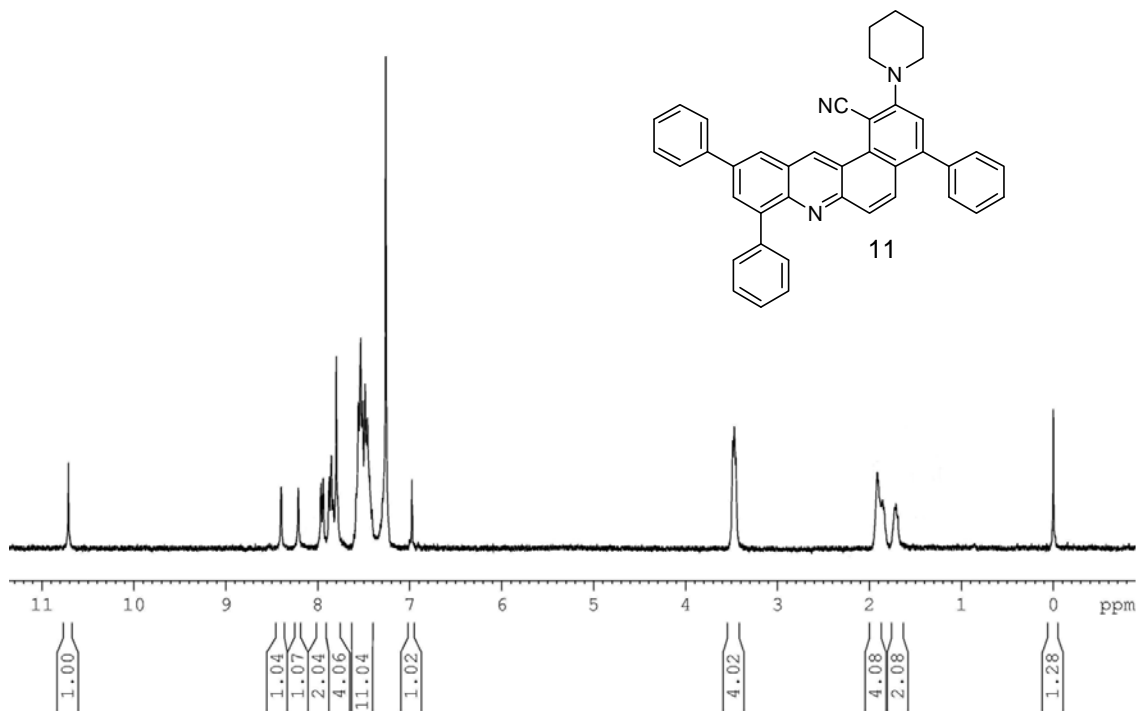


Figure 29. ¹H NMR spectrum of **11** in CDCl₃

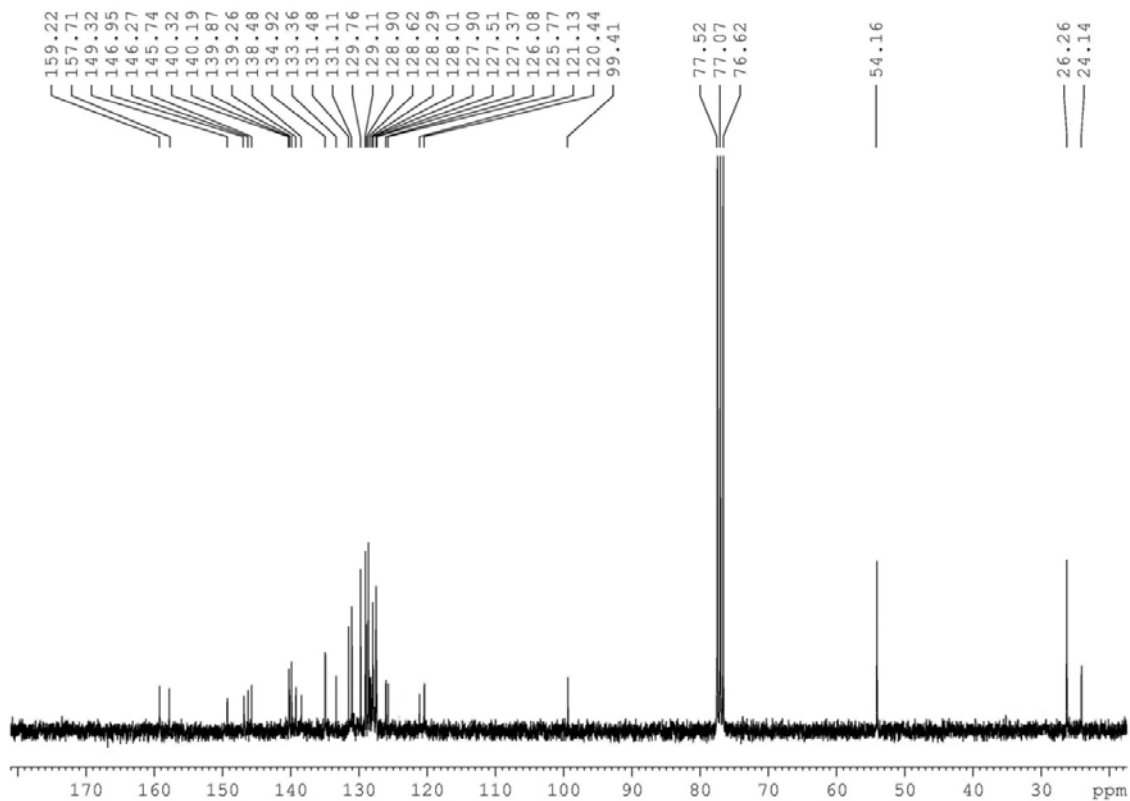


Figure S30. ¹³C NMR spectrum of **11** in CDCl₃